JOURNAL OF COMPUTATIONAL PHYSICS 73, 461–467 (1987)

Note

Weak Decay Processes in Lattice QCD*

I. Introduction

Many interesting phenomenological questions in weak interaction physics require the understanding of QCD corrections before an accurate comparison of theory to experiment is possible. While the basic theory describes pointlike interactions of quarks and weak gauge bosons, real world experiments provide us with data on the weak decays of confined multiquark bound states. Extraction of the phenomenological implications of the theory requires that one take into account hadron wavefunctions and binding effects. If QCD is the correct theory then it should be able to account for such effects.

In principle, the lattice formulation of QCD provides the theorist with a tool for performing finite nonperturbative calculations of strong interaction effects. However, actual lattice QCD calculations can range from small (a few hundred VAX hours) to prohibitively expensive (a few "Cray millenia" [1]) in computational resources. One of the arts of the field is to find interesting work that can be done with current state of the art computer technology.

One area of great interest to many workers is the detailed comparison of QCD predictions for hadron mass spectra with experiment. This work requires highly accurate determinations of the masses in QCD and serves both as a test of QCD and its lattice formulation. Success in this effort means the accurate determination of hadron masses given only $\Lambda_{\overline{\mathrm{MS}}}$ and quark masses as input. The principle difficulty that must be addressed in this work is the calculation of the effects of closed fermion loops. The inclusion of fermion loops requires computer time which grows like the square of the number of lattice sites—a gigantic computational effort.

In this paper, we consider a second area in which it is important and feasible to make progress with current and forthcoming computer technology: the calculation of matrix elements of weak currents between hadronic states. Accurate calculations of weak matrix elements will allow more precise testing of the Standard Model than has hitherto been possible. Precise testing of the Standard Model's implications for low-energy phenomena such as decay rates and mixing angles is one route to the verification of our understanding of weak physics and of the constraints phenomonology places on higher level unified theories.

The basic facts which make for this situation are:

* Given as a lecture in the 1986 TASI in Elementary Particle Physics, at the University of California, Santa Cruz, CA 95064.

0021-9991/87 $3.00

— There are weak amplitudes for which QCD effects lead to factors of 2–10 uncertainty. These include the $\Delta I = \frac{1}{2}$ rule [2], the $K^0\bar{K}^0$ mass splitting, proton decay in GUTS, CP violation, and the KM mixing matrix for heavy quarks. Accurate determination of these QCD effects can provide information important in testing the Standard Model and its extensions.

— Recent theoretical work by Bochicchio *et al.* [3] on the nature of chiral symmetry restoration and current algebra in the continuum limit of lattice theory with quenched Wilson fermions has eased the potential task of data analysis.

— There are techniques, such as the use of "extended source propagators" to compute propagator convolutions for processes involving spectator quarks, which allow for expeditious computation of matrix elements including momentum dependent effects as an adjustable parameter.

We describe a program of calculations which use quenched Wilson fermions and effectively local four-fermi weak interaction vertices. Our focus is on processes which require no further approximations for their analysis. In particular, we will not assume a priori PCAC or integrate out heavy quark fields. Quenching is not fundamental to our considerations except insofar as it saves computer time. Given a sample of thermalized lattices including fermion loop effects, one could apply all the same techniques of analysis.

II. Weak Matrix Elements

On lattices with lattice spacings a^{-1} on the order of 1 GeV, the propagation of heavy weak bosons can be handled using perturbative renormalization theory to take into account interactions on distance scales from the lattice spacing a down to the weak interaction scale $1/M_W$. The weak processes are described by matrix elements of local currents and current bilinears (four-fermi interactions).

There is a natural hierarchy of processes that can be calculated. It is convenient to classify them by the number of hadrons involved in the matrix element.

Leptonic Decays

Purely leptonic decays of mesons depend on matrix elements of the form: $\langle 0|\, J^\mu(0)\, |M, \mathbf{p}\rangle$, where $J^\mu(x)$ is one of the weak vector or axial vector currents and $|M, \mathbf{p}\rangle$ represents a meson state of momentum $\mathbf{p}$. The state $|M, \mathbf{p}\rangle$ can be created by a quark–antiquark operator. For example, a zero momentum meson decay matrix element would be represented in configuration space by the quantity (Fig. 1a)

$$M_\Gamma(T) = \sum_{\mathbf{x}} \langle 0|\, \bar{\Psi}(\mathbf{x}; -T)\, \Gamma \Psi(\mathbf{x}; -T)\, J_\mu(0)\, |0\rangle, \tag{1}$$

where Γ gives the appropriate flavor spin combination and the sum over spacial positions guarantees $\mathbf{p} = 0$. (See Fig. 1a.) The amplitude $M_\Gamma(T)$ must be averaged over gauge field configurations. Processes of this class have been studied by several

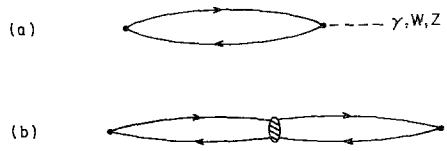

FIG. 1. Class 1 diagrams: (a) meson decay, (b) meson mixing ($K^0\bar{K}^0$, for example).

groups, notably by Maiani and Martinelli [4] in the context of their lattice current algebra work [3].

The calculation of the above matrix element for any combination of weak currents and Γ requires knowledge of the Dirac propagator from the origin to each point in the space-time lattice. To quantify the calculation efforts of these problems, it is convenient to refer to the number of "inversions" in finding solutions to a linear system of the form:

$$\sum_{j,b,x'} \mathscr{D}_{ia,jb}(x, x')\, \Psi_{jb}(x') = j_{ia}(x), \tag{2}$$

where $\mathscr{D}_{ia,jb}(x, x')$ is the lattice Dirac operator for a single Wilson fermion flavor, and $j_{jb}(x')$ is a source with spin index j and color index b. One such inversion corresponds to a single Gauss–Seidel or conjugate-gradient operation. Calculation of the whole propagator from the origin ($D_{ia,jb}(x, 0) = \mathscr{D}^{-1}_{ia,jb}(x, 0)$) requires 12 inversions, one for each possible flavor-spin delta source $j_{jb}(x') = \delta_{j,j_0}\delta_{b,b_0}\delta(x')$. The calculations of these leptonic decays can be done as a by-product of the quenched mass calculations since the inverse data required is the same.

The extraction of the contribution of the desired meson state $|M, \mathbf{0}\rangle$ can be done by fitting the T dependence of the gauge averaged $M_\Gamma(T)$ to the appropriate sum of exponentials[1]

$$\langle\langle M_\Gamma(T)\rangle\rangle = \sum_\alpha \langle 0|\, \bar{\Psi}\Gamma\Psi\, |\alpha\rangle\, e^{-m_\alpha T}\, \langle\alpha|\, J_\mu(0)\, |0\rangle, \tag{3}$$

where the sum is over all possible intermediate states α with the right quantum numbers.

Normalized current matrix elements require wavefunction normalization constants $\langle 0|\, \bar{\Psi}\Gamma\Psi\, |\alpha\rangle$ which can be extracted (somewhat less reliably) from the fit to the T dependence of the meson propagator itself. It is interesting to note that relative matrix elements involving the lowest mass state in a given color-spin channel can be estimated simply by measuring masses and the above matrix elements for a single sufficiently large T.

The one hadron processes described here require the same number of inversions as the mass determination. Another group of processes which are also of this order of difficulty are those with internal weak interactions and no momentum transfer (see Fig. 1b). Typically these processes involve further theoretical approximations to be cast in the local form. Examples are:

[1] The contribution of spurious time wrapped states has been omitted for convenience of exposition.

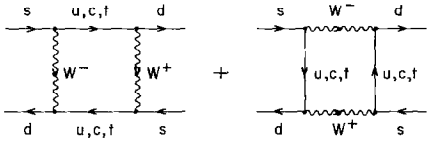

FIG. 2. $K^0\bar{K}^0$ mixing "local" kernel.

1. The $\Delta I = \frac{1}{2}$ rule matrix elements after PCAC has been invoked to remove one of the two π's in $K \to \pi\pi$. The effect here is very large, but the theoretical situation is complicated by operator mixing, the accuracy of PCAC, and the important contribution of the "eye" graph or nonlocal penguin graph.

2. The $K^0\bar{K}^0$ mass splitting using a local effective Hamiltonian approximation. Here, the local "blob" in Fig. (1b) is the effective Hamiltonian which involves the exchange of a pair of W's and the integration over c, u, and t quarks (Fig. 2).

Semi-leptonic Decays

Semi-leptonic decays and form-factors of mesons and baryons are two hadron processes. Proton decay also falls in this class. (See Fig. 3.) The essential ingredient which distinguishes these processes is that there are one or more "spectator" quarks which propagate between the initial and final points without touching the interaction vertex.

For example, the diagram (Fig. 3a) for the semi-leptonic decay of a meson has the form of the following convolution of propagators:

$$\mathcal{A}^x(T, x_f) = \sum_{x_i} \sum_{a,b,c} \sum_{k,l,m,n} \Psi^f_{ij} D^1_{ja,kb}(x_f, 0)\, J^x_{kl} D^2_{lb,mc}(0, x_i) \times \Psi^i_{mn} D^3_{nc,ia}(x_i, x_f) \tag{4}$$

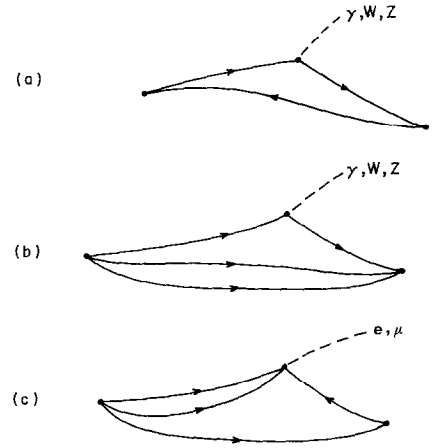

FIG. 3. Semileptonic decay graphs: (a) meson, (b) baryon, (c) proton decay.

where, Ψ_{ij}'s are the meson spin wavefunctions and J^{α}_{ij} are the spin matrix elements of the weak current α. The propagators D^1, D^2, and D^3 are Wilson fermion propagators of (possibly) different flavors. As before, the sum over spatial positions of the initial meson state (with $x_i^0 = -T$) projects out the $\mathbf{p} = \mathbf{0}$ component. We have taken the weak vertex to be at the origin.

The amplitude requires knowledge both of the propagator from the origin to elsewhere in space and the propagator for the spectator quark directly from the initial to the final state. It might then appear that one needs many more inversions—a whole time plane full ($12L^3$) to perform a full convolution over $\mathbf{x}_i$. Fortunately, this can be avoided by using the "extended source propagator" (ESP) technique [5]. This amounts to the observation that for each color-spin component *lb*, the convolution:

$$\mathscr{F}^{\dagger}_{ia}(x_f) \equiv \sum_{\mathbf{x}_i} \sum_{c,m,n} D^2_{lb,mc}(0, x_i)\, \Psi^i_{mn} D^3_{nc,ia}(x_i, x_f) \tag{5}$$

is the solution of

$$\sum_{\mathbf{x}_i} \sum_{ia} D^3_{nc,ia}(x_f, x_i)\, \mathscr{F}_{ia}(x_i) = \sum_{m} \Psi^{i\dagger}_{nm} D^{2\dagger}_{mc,lb}(x_i, 0). \tag{6}$$

The right-hand side of this equation is the "extended source." Calculation of $\mathscr{F}$ requires 12 inversions (like a propagator) and amounts to doing the convolution before the inversion.

With this trick, only $3 \times 12 = 36$ inversions per initial spin state are needed even in the worst case of different mass quarks on all three legs of the diagram.

The result of this work is a calculation of the amplitude $\mathscr{A}$ connecting a $\mathbf{p} = \mathbf{0}$ meson state of definite spin created at time $-T$ to a weak decay vertex at $x = 0$ with observation of the final state $q\bar{q}$ pair at any point x_f in space-time. This data allows for momentum and energy analysis on the final state. In order to extract the contribution of a pure initial state meson, the calculation must be repeated for a variety of T values or, with less reliability, the lowest state in the $\mathbf{p} = \mathbf{0}$ channel may be assumed to dominate.

A similar method will work for the baryonic diagrams (Figs. 3b and 3c). In these cases, the sources are constructed from di-quarks and the baryonic spin wavefunction. There are also more spin-flavor combinations to be considered.

Two-body Hadronic Decays

Two-body hadronic decays involve three hadron matrix elements. These include nonleptonic decays. The diagrams of interest involve spectators which can be treated by the extended source propagator method described above. Additionally, these processes can involve spectators (Figs. 4a and 5) and/or exchange and annihilation (Fig. 4b) channels. Also the "eye" graphs (Fig. 6) of the $K \to \pi\pi$ amplitude, which is of interest for $\Delta I = \frac{1}{2}$, falls into this class when the assumption of PCAC is not used.

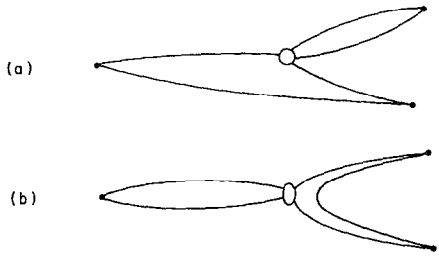

FIG. 4. Nonleptonic two-body decay graphs: (a) spectator, (b) exchange and annihilation.

Typical processes in this class usually involve more inversions than class 2, but they are also approachable with a single extended source propagator for one of the external hadrons. In addition, these processes require extraction of hadronic states on all three legs. Therefore, they are expected to have larger errors from finite size effects and from statistics. Nonetheless, for specific channels either the number of inversions can be comparable to the semileptonic decays, or the experimental results better determined such that the purely hadronic channel is preferable. Much detailed phenomenology remains to be done to clearly identify the best channels. The totality of a computationally feasible decay channel is somewhat daunting.

III. COMPUTATIONAL CONSIDERATIONS

The computational environment needed to begin the program of computations described in this paper is one equivalent to a state of the art vector supercomputer, e.g., the CDC CYBER 205. As described, the program starts by performing calculations of difficulty comparable to that of the quenched mass spectrum. Since many inversions can be used for a variety of processes and matrix elements, there is considerable potential for re-use of the inverse data.

Our work is to be done using time-doubled versions of existing thermalized $16^3 \times 32$ lattices of Moriarty, Rebbi, and Samuel. We expect that times of order 500–1000 CYBER 205 h will allow a significant impact in these areas.

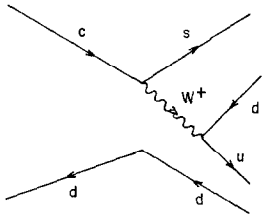

FIG. 5. Spectator graph for $D^+ \to K^0\pi^+$.

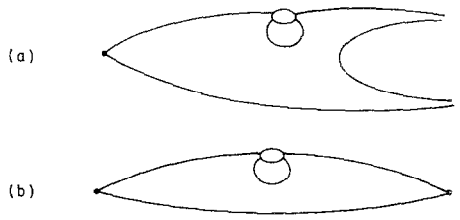

FIG. 6. Eye graphs for $K \to \pi\pi$: (a) class 3 graph, (b) PCAC approximation (class 2).

ACKNOWLEDGMENTS

We would like to thank Robert M. Price, Larry Jodsaas, and Lloyd M. Thorndyke for their continued interest, support, and encouragement and access to the CYBERNET CDC CYBER 205 at Rockville, Maryland; the Consortium for Scientific Computing for access to the CYBER 205 at Princeton, New Jersey; the Control Data Corporation for the PACER Fellowship Grants 85PCR06 and 86PCR01 for financial support, and the Natural Sciences and Engineering Research Council of Canada for Grant NSERC A9030 for further financial support.

REFERENCES

1. J. KOGUT, unpublished.
2. N. CABIBBO, G. MARTINELLI, AND R. PETRONZIO, *Nucl. Phys. B* **244**, 381 (1984); R. C. BROWER, G. MATURANA, M. B. GAVELA, AND R. GUPTA, *Phys. Rev. Lett.* **53**, 1318 (1984); C. BERNARD, T. DRAPER, G. HOCKNEY, A. M. RUSHTON, AND A. SONI, *Phys. Rev. Lett.* **55**, 2770 (1985).
3. M. BOCHICCHIO, L. MAIANI, G. MARTINELLI, G. ROSSI, AND M. TESTA, *Nucl. Phys. B* **262**, 331 (1985).
4. L. MAIANI AND G. MARTINELLI, *Phys. Lett. B* **178**, 265 (1986).
5. This technique was used independently by authors of reference [4].

RECEIVED: September 12, 1986

RICHARD C. BROWER

Physics Department and Department of Electrical, Computer and Systems Engineering, Boston University, Boston, Massachusetts 02215

ROSCOE GILES

Department of Electrical, Computer and Systems Engineering, Boston University, Boston, Massachusetts 02215

K. J. M. MORIARTY

Consortium for Scientific Computing, John von Neumann Center, 665 College Road East, Princeton, New Jersey 08543